Supplementary Information

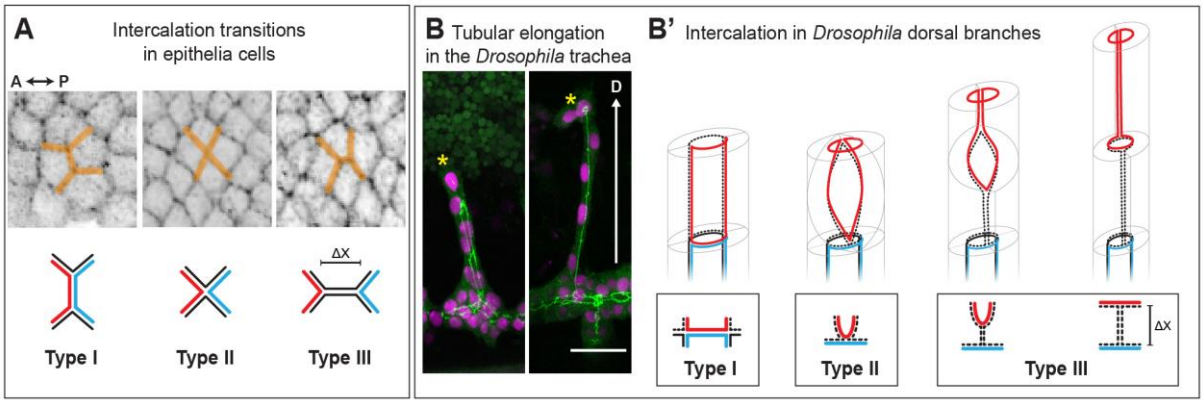

Supplementary Figure 1 – Cell intercalation in flat and tubular epithelia follows similar geometric rules
(A**)** Anteroposterior (A-P) elongation of the germ-band in the early *Drosophila* embryo is caused by the intercalation of hexagonal cells. During intercalation and tissue extension junctions remodel in a stereotypic and ordered manner, characterized by three irreversible transitions: Shrinkage of cell contacts between anterior-posterior neighbors (red and blue cell, type I) is followed by new contact formation between dorsal and ventral neighboring cells (black cells, type II). This novel cell-cell contact is expanded (Δx) along the anterior-posterior axis, resulting in net tissue elongation along this axis (type III). (B) Tubular elongation in the *Drosophila* tracheal system. The dorsal branches elongate dorsally (D, see arrow) owing to the migratory behavior of the tip cells (stars) (nuclei in pink, junctions in green). Intercalation in dorsal branches (B'): Pairs of cells remodel their junctions (dotted black and red) during intercalation resulting in a chain-like arrangement of cells after completion of the process. Junction remodeling is polarized and follows a stereotyped pattern corresponding to a type I to type II transition, and junction expansion, corresponding to a type II to type III transition as observed in germ-band extension.

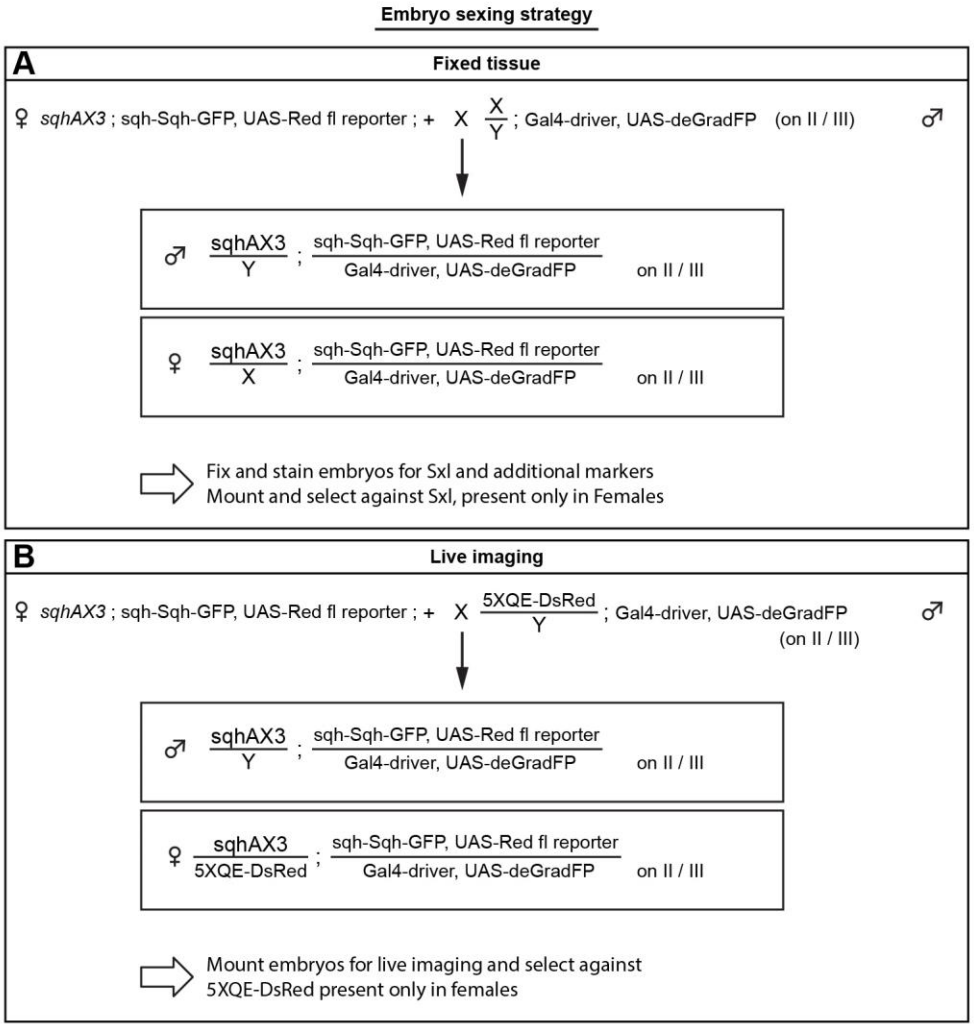

Supplementary Figure 2 - Embryo sexing strategy

In general, experimental embryos were generated by crossing *sqhAX3*; *sqh-Sqh- GFP, UAS-Red fluorescent reporter* females to *sqh+*/Y; *Gal4 driver and UAS-deGradFP* (on the second / third chromosome) males. In the male progeny, the only source of Sqh was *sqh-Sqh-GFP*, whereas in female progeny a copy of *sqh+* was still present (provided by the X chromosome from the male). Control embryos were generated by crossing *sqhAX3*; *sqh-Sqh-GFP, UAS-Red fluorescent reporter* females to *sqh+*/Y; *Gal4 driver* (on second / third chromosome). (A) In fixed samples the gender of the embryos was identified by staining for and selecting against the female specific factor Sxl. (B) For the live imaging experiments a red fluorescent transgene (*5XQE-DsRed*) on the X chromosome of the parental males allowed us to distinguish and select against the female.

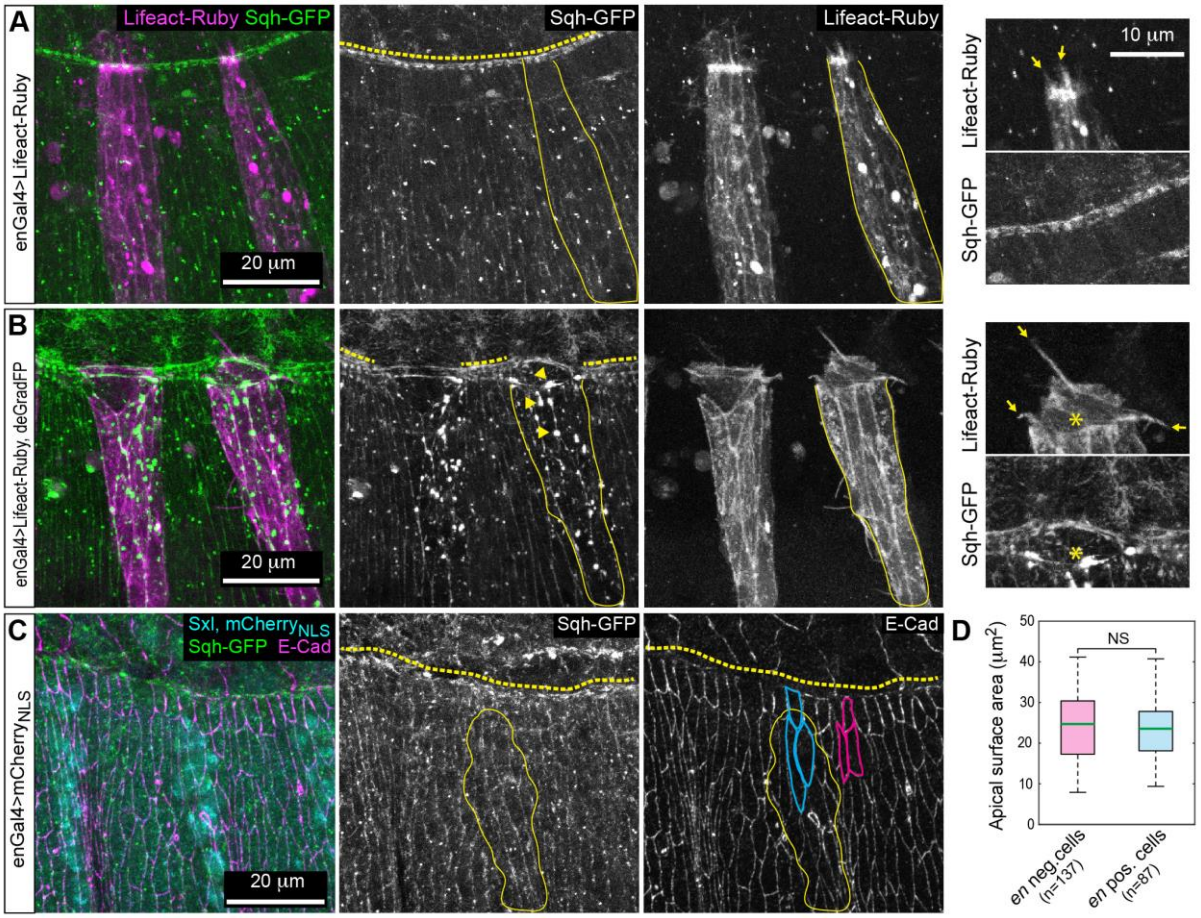

Supplementary Figure 3 – deGradFP-mediated Sqh-GFP knock-down in epidermal cells

All panels show lateral views of stage 14 male *sqhAX3*; *sqh-Sqh-GFP* embryos additionally expressing the indicated transgenes in the engrailed (*en::Gal4*) stripe pattern. Representative *en* stripes are highlighted by continuous yellow lines. (A,B) Live imaging revealed that in control embryos (A) Sqh-GFP localizes in small punctuae at the cell cortex and forms a continuous actomyosin cable (yellow dashed line). In contrast, in deGradFP expressing embryos Sqh-GFP coalesces prominently at the cortex forming large spots (arrowheads in (B) middle) and the dorsal actomyosin cable is lost in the *en* stripes. Also, deGradFP expressing embryos formed more and longer filopodia at the leading epidermal edge visualized by Lifeact-Ruby (compare arrows in A and B right). (C) Male control embryo stained for E-Cad (magenta). A dotted yellow line marks the leading epidermal edge and a continuous yellow line highlights a representative en stripe. In control embryo similar apical cell surface in the *en* positive cells (blue outlines) and in the *en* negative cells (pink outlines) are observed. (D) Quantification of apical cell surface area of cells inside (blue) and outside (pink) of the *en* stripe. The green lines mark the median; whiskers correspond to minimum and maximum data points. Statistical significance was assessed using a two-sided Students *t-test* (p=0.22).

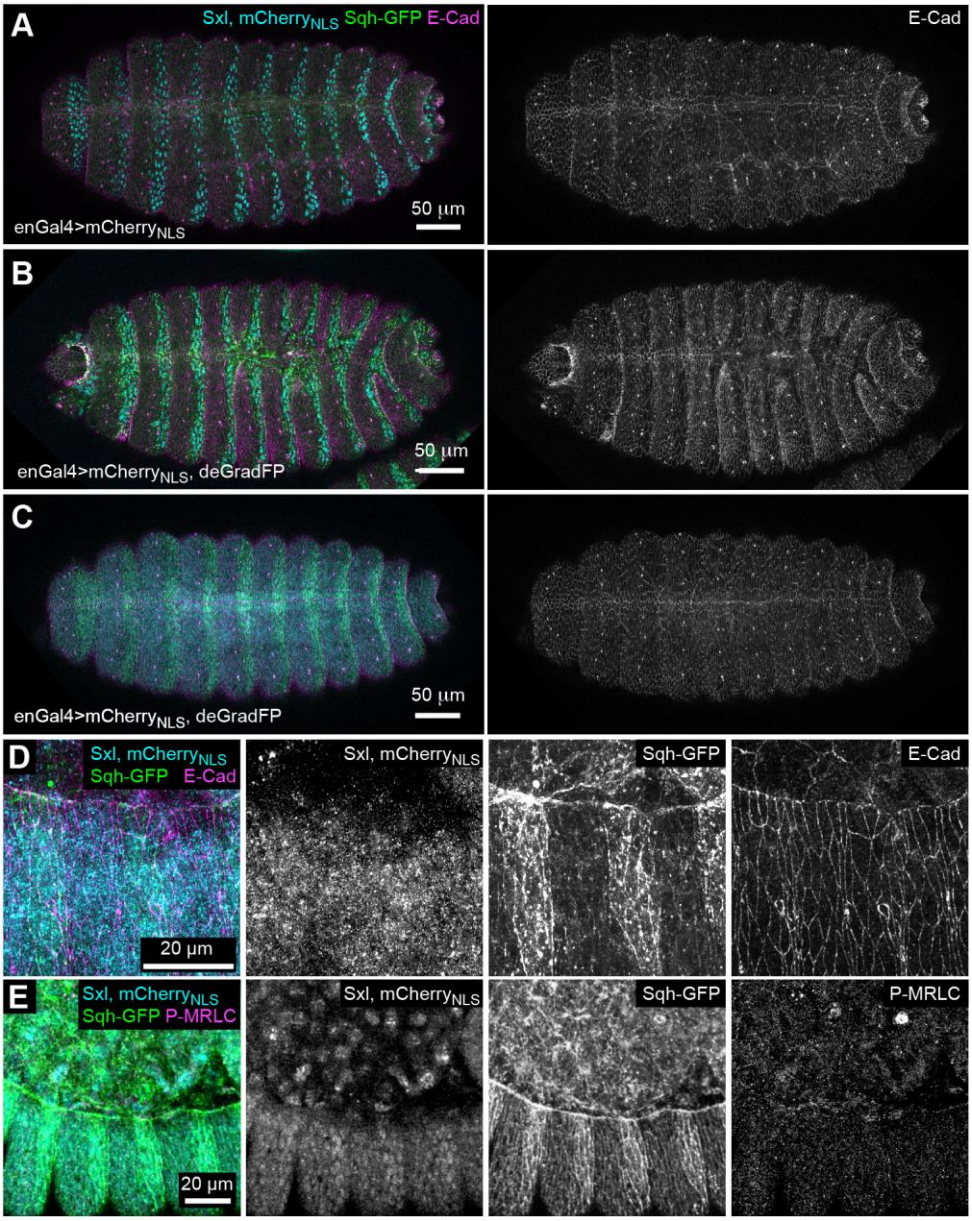

Supplementary Figure 4 – Dorsal closure in epidermal Sqh-GFP knock-down embryos

(A-C) Dorsal views of stage 16 embryos stained for Sxl and E-cad of the following genotypes: (A) *sqhAx3*/Y; *sqh-Sqh-GFP*/*en-Gal4*, *UAS-mCherry$_{NLS}$*, (B) *sqhAx3*/Y *sqh-Sqh-GFP*/*en-Gal4*, *UAS-mCherry$_{NLS}$*; *UAS-deGradFP*/+, (C) *sqhAx3*/*sqh+*; *sqh-Sqh-GFP*/*en-Gal4*, *UAS-mCherry$_{NLS}$*; *UAS-deGradFP*/+. While control embryos and female embryos expressing deGradFP have a normal epithelial architecture and normal dorsal closure (A, C), male embryos expressing deGradFP (B) manage to close dorsally but all deGradFP expressing stripes show bigger apical cell area and seal aberrantly with the contralateral stripes. (D-E) Lateral views of stage 14 female embryos with genotype *sqhAx3*/*sqh+*; *sqh-Sqh-GFP*/*en-Gal4*, *UAS-mCherry$_{NLS}$*; *UAS-deGradFP*/+, stained for anti-Sxl and anti-E-Cad (D) and stained for anti-Sxl and anti-P-MRLC (E). See Fig.1A and Fig.S3C for comparison. Female embryos carry one wt and one mutant copy of *sqh* (*sqhAX3*) in addition to one rescue *sqh-Sqh-GFP* transgene and express deGradFP in *en* stripes. Like in controls (Fig.1A), these embryos form a continuous actomyosin cable at the lateral and leading edge epithelium. However, unlike control embryos, Sqh-GFP in female deGradFP embryos shows aberrant bulky accumulation in *en* stripes similar to male deGradFP embryos (Fig.1C). Nonetheless female deGradFP embryos show uniform epithelial P-MRLC distribution with enrichment at the actomyosin cable (E) and give rise to viable flies.

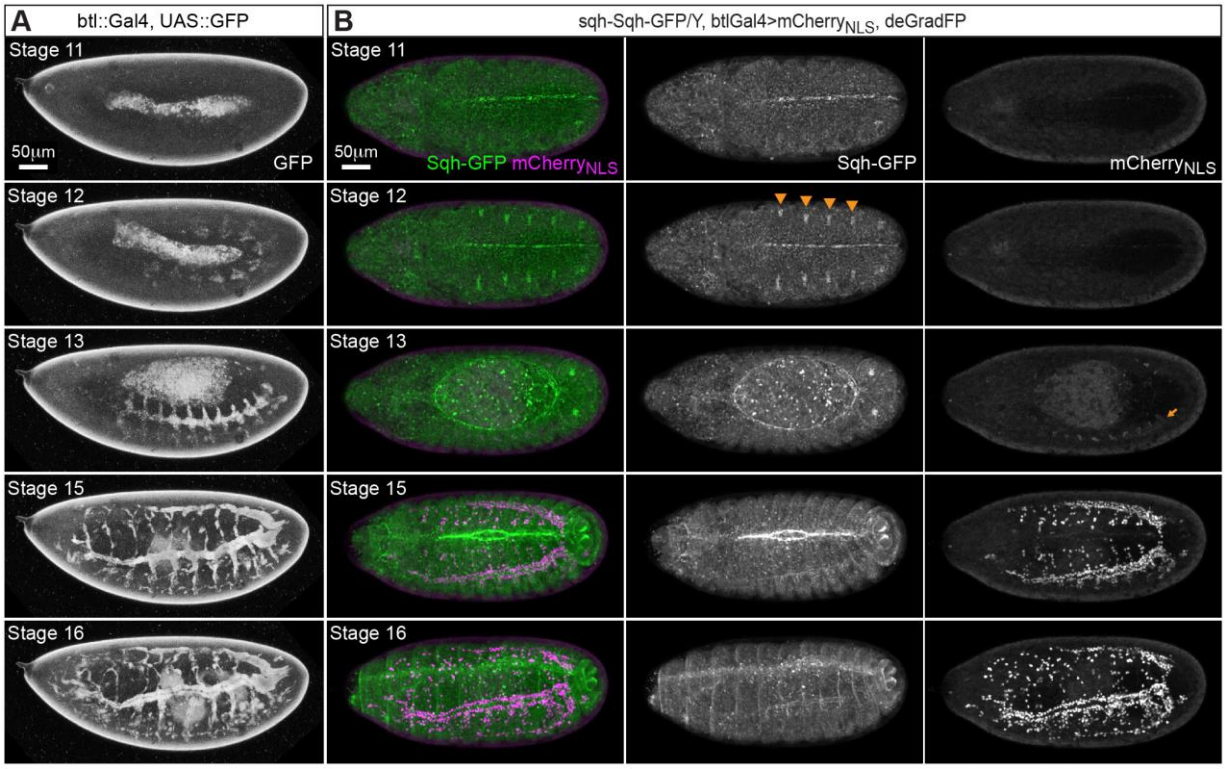

Supplementary Figure 5 – Temporal activity of the *btl-Gal4* driver line

(A), Stills from a movie of a *btl-Gal4, UAS-GFP* embryo, the respective embryonic stages are indicated (lateral views). GFP expressed under the control of *btl-Gal4* can be detected form stage 12 onward in the tracheal system. At earlier stages (stage 11) we did not detect GFP fluorescence in tracheal cells. At stage 13, before the start of DB elongation, high levels of GFP are detected in tracheal cells. (B) Panels show dorsal views of male *sqhAX3*; *sqh-Sqh-GFP* embryos expressing mCherry$_{NLS}$ together with deGradFP (Stills from Movie 1). Consistent with the results shown in (A), we start detecting the spotted accumulation of Sqh-GFP (indicating deGradFP activity) at stage 12 (see orange arrowheads). However, we do not detect Sqh-GFP accumulation at earlier time points (top row). This result shows that *btl-Gal4* induces deGradFP expression early enough to effectively inhibit Sqh function at stage 13-15 when DB elongation takes place. Interestingly, we only detected mCherry signal at embryonic stage 13 (see arrow), while GFP was already detectable at stage 12 when expressed under *btl-Gal4*. This difference might be due to the longer maturation time of mCherry compared to GFP and suggests that GFP (see A) better represents the temporal activity of the *btl-Gal4* driver line.

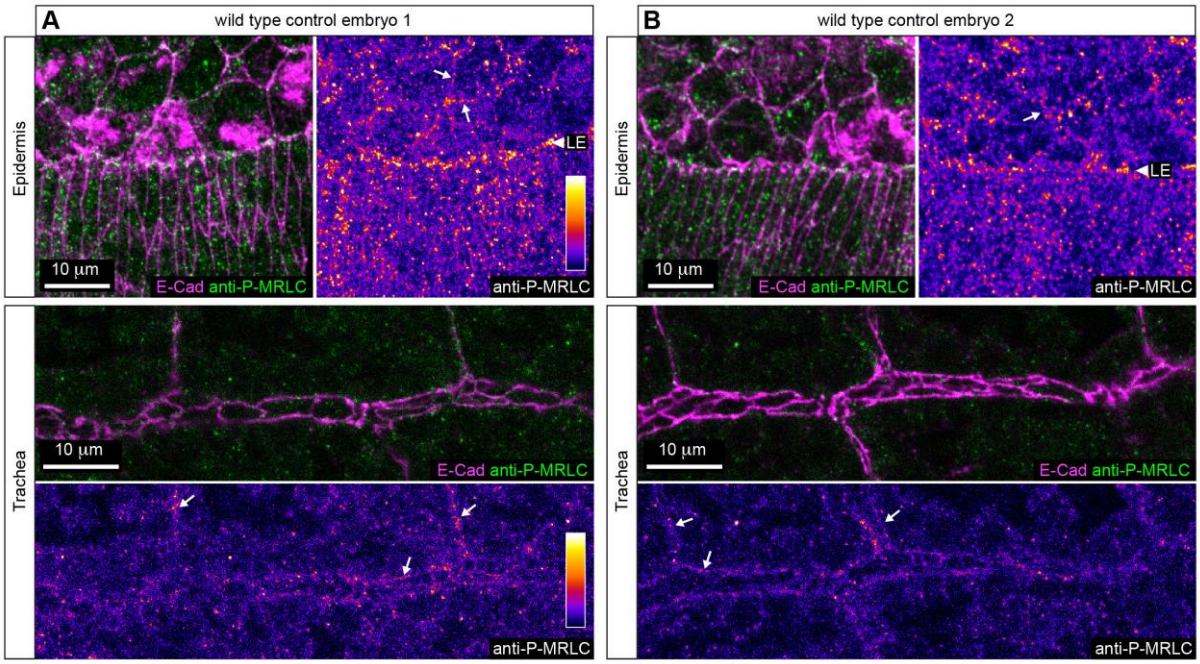

Supplementary Figure 6 – P-MRLC staining in wild type embryos

(A,B) Two representative wild type embryos stained for E-Cadherin (magenta) and P-MRLC (green/false-color). (top) Strong P-MRLC signal is observed at the Myosin cable forming along the leading edge (LE, arrowhead) of epidermal cells during dorsal closure. P-MRLC staining is also observed along the junctions of amnioserosa cells (white arrows). (bottom) Also in the tracheal system low but rather diffuse levels of P-MRLC signal can be observed along the tracheal cell junctions (white arrows).

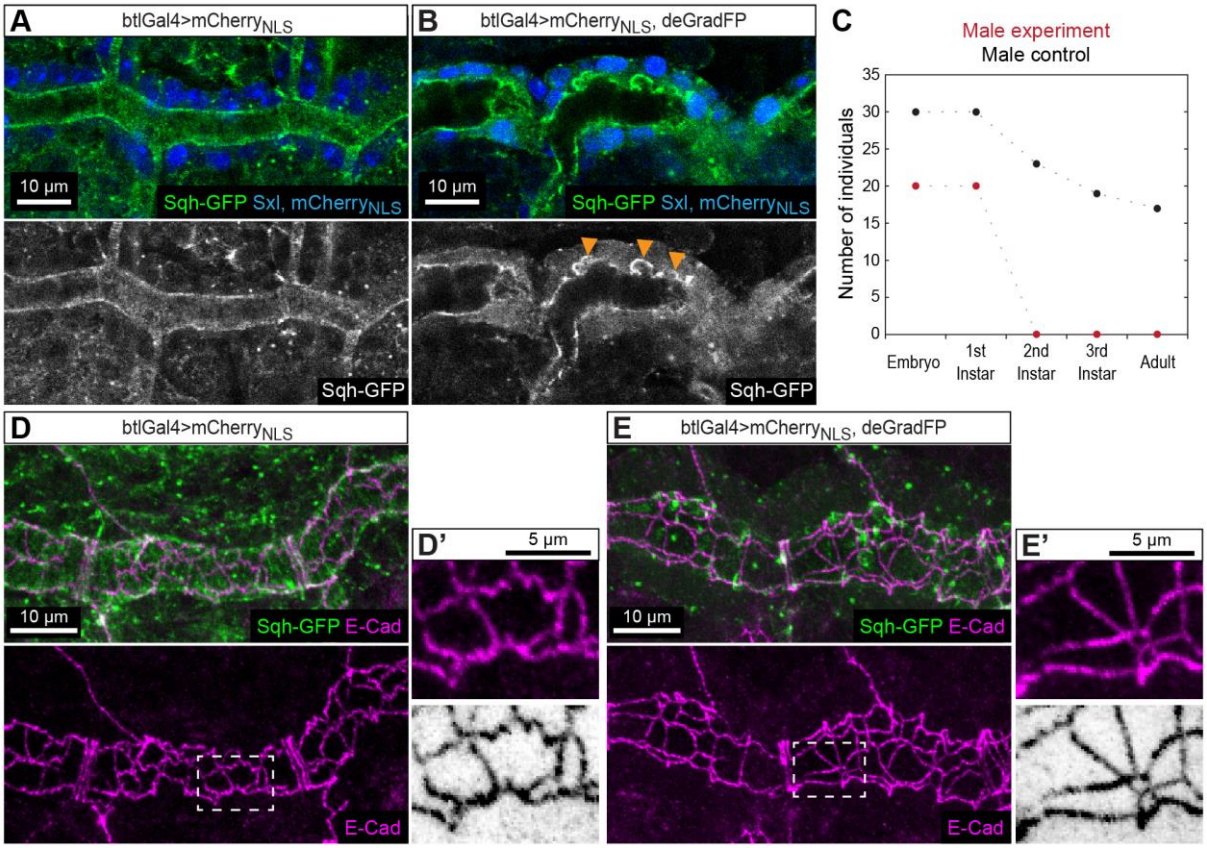

Supplementary Figure 7 –Sqh-GFP knock-down results in alteration of dorsal trunk morphology

(A-B) Dorsal trunk of late stage 16 *sqhAX3*; *sqh-Sqh-GFP* embryos expressing $mCherry_{NLS}$ (A, control) or $mCherry_{NLS}$ together with deGradFP (B) in the tracheal system (*btl-Gal4*). While in control embryos the surface of the dorsal trunk is smooth, the surface of the dorsal trunk of Sqh-GFP knock-down embryos can be rough with excrescences forming (yellow arrowheads). Also the diameter of the dorsal trunk of Sqh-GFP knock-down embryos shows more variation and tends to be increased compared to control embryos. (C) Lethality of male *sqhAX3*; *sqh-Sqh-GFP* embryos (Male Control, black) compared to male *sqhAX3*; *sqh-Sqh-GFP* embryos expressing deGradFP in tracheal cells (Male experiment, red). Sqh-GFP knock-down results in larval lethality at the early second instar stage. (D-E) Male *sqhAX3*; *sqh-Sqh-GFP* embryos expressing $mCherry_{NLS}$ (D, control) or $mCherry_{NLS}$ together with deGradFP (E) in the tracheal system (*btl-Gal4*) and stained for E-Cad (magenta). In control embryos tracheal junctions show a wriggled appearance (D, see also magnification in D'). In contrast, in Sqh-GFP knock-down embryos tracheal junctions are less wriggled but have a linear appearance. This observation together with the increase in dorsal trunk diameter suggests that MyoII function is required for proper control of tracheal tube morphology at late embryonic stages as suggested previously (Kato et al., 2016).

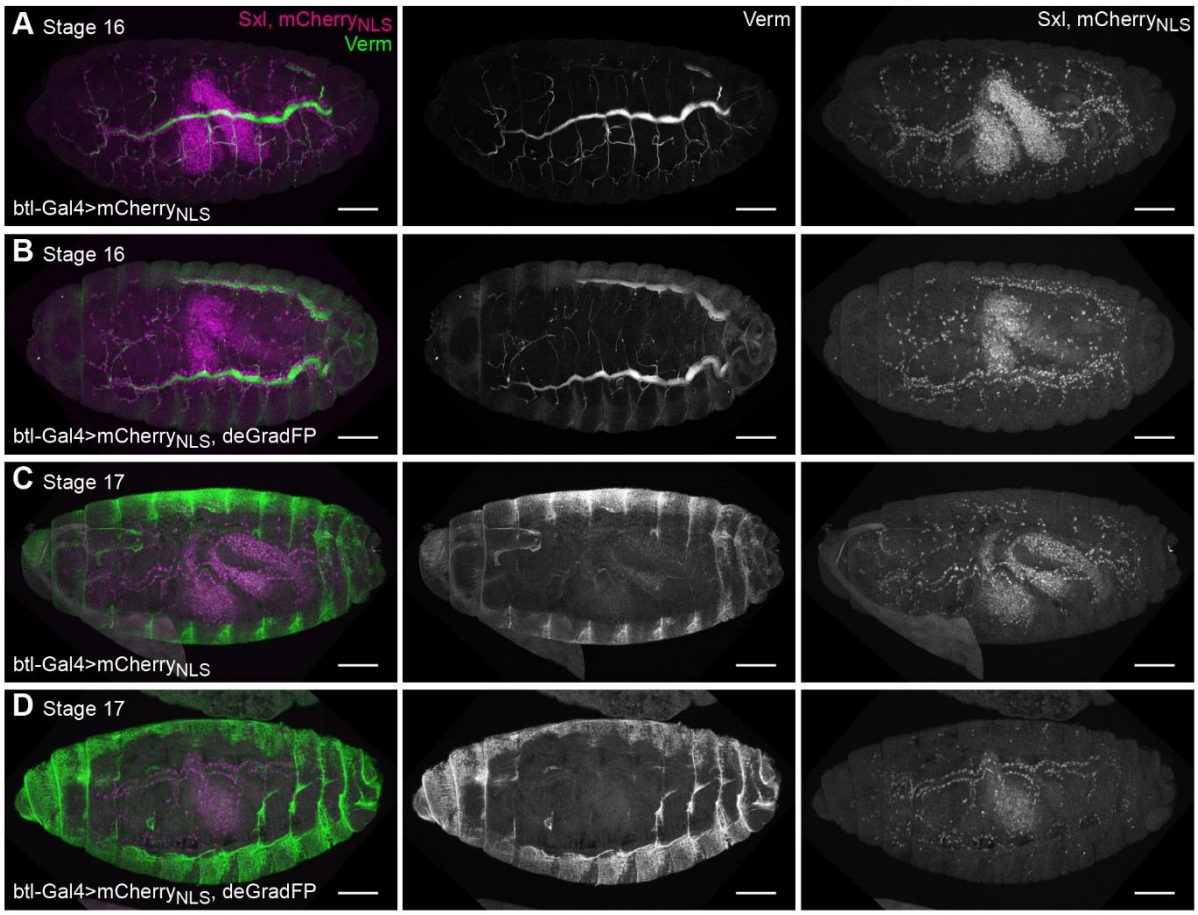

Supplementary Figure 8 – Deposition and clearance of Vermiform (Verm) does not require MyoII

Panels show dorsolateral views of male *sqhAX3*; *sqh-Sqh-GFP* embryos expressing mCherry$_{NLS}$ (A and C, control) or mCherry$_{NLS}$ together with deGradFP (B and D) in the tracheal system (*btl-Gal4*) and stained for Sxl and Verm. The secretion of Verm into the tracheal lumen (A and B, stage 16) and ensuing Verm clearance (C and D, stage 17) in knock down embryos is indistinguishable from male control embryos. GFP channel is not shown. Scale bar is 50µm.

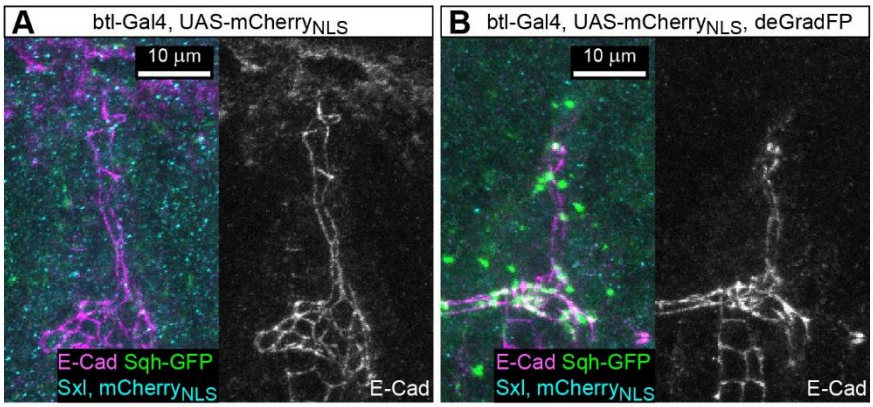

Supplementary Figure 9 – DB cell constellation prior to SCI in Sqh knock-down embryos

DBs of stage 13 male embryos prior to SCI stained for and E-Cad (magenta). Both, control (*sqhAx3*/Y; *sqh-Sqh-GFP, btl-Gal4, UAS-mCherry$_{NLS}$*/+) and tracheal specific Sqh-GFP knock-down embryos (*sqhAx3*/Y; *sqh-Sqh-GFP, btl-Gal4, UAS-mCherry$_{NLS}$/UAS-deGradFP*) show intercellular junctions between opposite facing cells. mCherry NLS expression is weak at this stage, however spotted accumulation of Sqh-GFP denoting deGradFP activity is clearly visible in knock-down embryos.

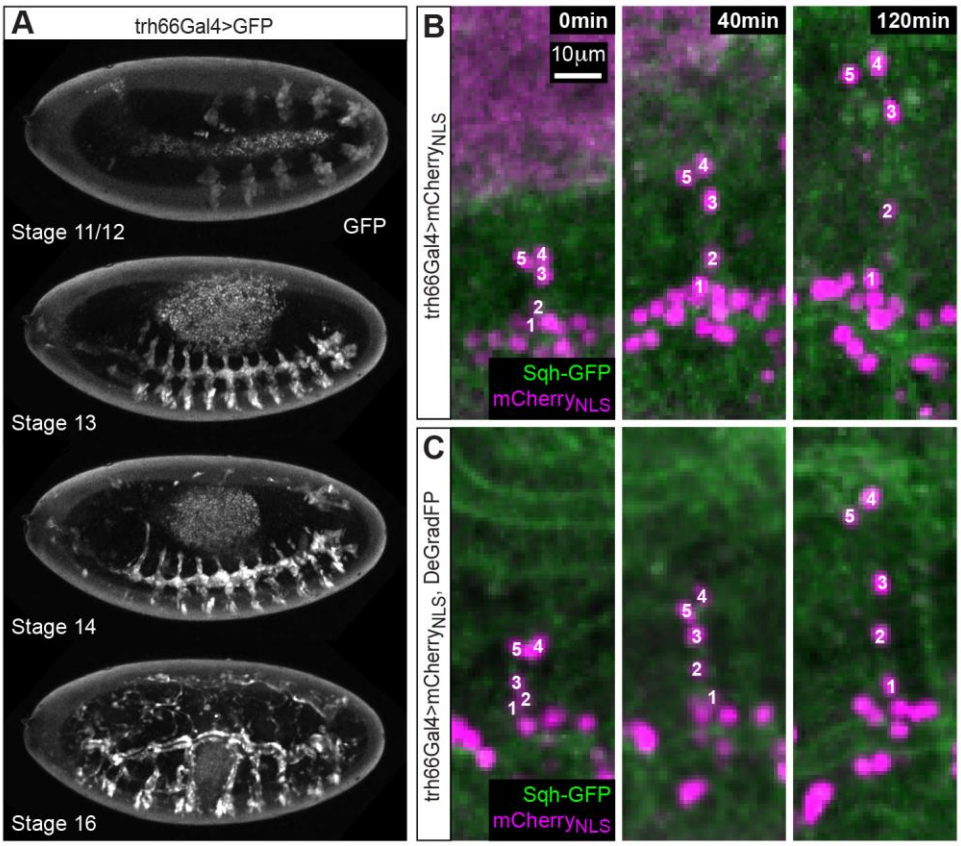

Supplementary Figure 10 – Sqh-GFP knock-down using *trachealess-Gal4* does not impair DB elongation

(A) Stills from a time laps movie of an embryo expressing GFP under the control of trachealess-Gal4 (*trh-Gal4*). Trh-Gal4 already drives expression of GFP at stages 11/12 (top). High expression levels are observed at stage 14, shortly before DB elongation and SCI. (B-C) Panels show stills from time laps movies of DB elongation in male *sqhAX3*; *sqh-Sqh-GFP* embryos expressing either $mCherry_{NLS}$ (B) or $mCherry_{NLS}$ together with deGradFP (C) in the tracheal system (*trh-Gal4*). Elongation of DBs (individual cells are numbered) in Sqh-GFP knock-down embryos (C) occurred indistinguishable to control DBs (B).

effector	genotype	DC	lethality
deGradFP	$\frac{sqh^{AX3}}{Y}$; $\frac{sqh::GFP}{Gal4^{332.3}}$; $\frac{UAS\_deGradFP}{+}$	open	embryonic
zip-GFP.DN	$\frac{Gal4^{332.3}}{+}$; $\frac{UAS\_zip.GFP.DN}{+}$	WT	semi lethal few adult escapers
rok.Cat-KG^{2B1}	$\frac{Gal4^{332.3}}{UAS\_rok.CAT\text{-}KG^{2B1}}$	ND	none
rok.Cat-KG^{3}	$\frac{Gal4^{332.3}}{+}$; $\frac{UAS\_rok.CAT\text{-}KG^{3}}{+}$	ND	none
TRiP.HMS01618 (against zip) (Valium 20)	$\frac{Gal4^{332.3}}{+}$; $\frac{TRiP.HMS01618}{+}$	ND	L2 ⟶ L3
TRiP.GL00623 (against zip) (Valium 22)	$\frac{Gal4^{332.3}}{TRiP.GL00623}$	ND	pupal
TRiP.HMS00437 (against sqh) (Valium 20)	$\frac{Gal4^{332.3}}{+}$; $\frac{TRiP.HMS00437}{+}$	ND	L1 ⟶ early L3
TRiP.HMS00830 (against sqh) (Valium 20)	$\frac{Gal4^{332.3}}{+}$; $\frac{TRiP.HMS00830}{+}$	ND	pupal
TRiP.GL00663 (against sqh) (Valium 22)	$\frac{Gal4^{332.3}}{TRiP.GL00663}$	ND	none
Rho1.N19	$\frac{Gal4^{332.3}}{+}$; $\frac{UAS\_Rho1.N19}{+}$	ND	none

Supplementary Table 1 - Tissue specific Myo II functional knock-down methods assayed on dorsal closure

Effector lines interfering directly with Myosin II components, its regulators, or RNAi lines directed at mRNAs of Myosin II components. Genotypes of embryos expressing such lines driven by the amnioserosa driver Gal4 332.3 and the dorsal closure (DC) phenotypes observed: open (amnioserosa exposed), WT (wild type), ND (not determined) due to non-lethality or larval to pupal lethality.

Movies

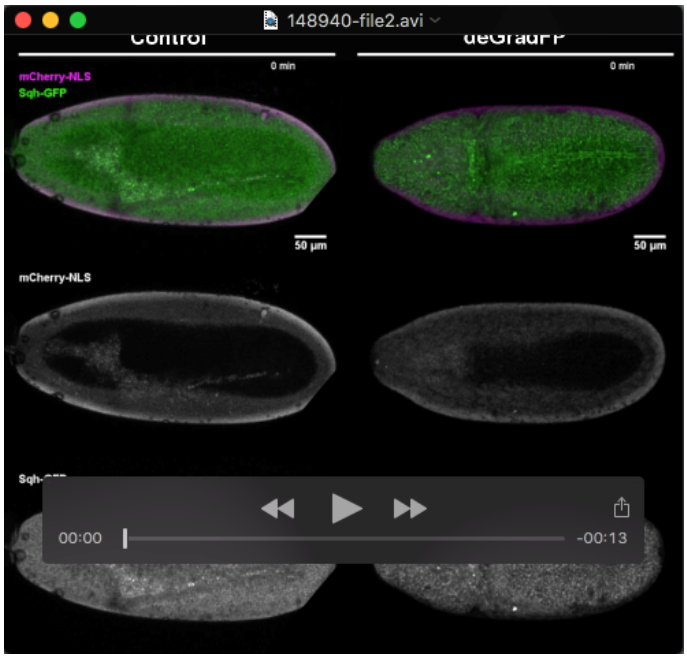

Movie 1 – The *Drosophila* trachea system forms normally in the absence of MyoII function

Time lapse imaging of *sqhAx3*/Y; *sqh-Sqh-GFP, btl-Gal4, UAS-mCherry$_{NLS}$*/+ control (left) and *sqhAx3*/Y; *sqh-Sqh-GFP, btl-Gal4, UAS-mCherry$_{NLS}$*/*UAS-deGradFP* Sqh-GFP knock-down (right) embryos (10min intervals, 20x objective). deGradFP expression resulted in the spotted accumulation of Sqh-GFP (green, right top panel), indicating deGradFP activity and effective inactivation of MyoII function. Labelling of trachea nuclei by mCherry$_{NLS}$ (*btl::Gal4*) shows that despite knock-down of MyoII function in tracheal cells development of the tracheal system is not impaired compared to the control embryo (left).

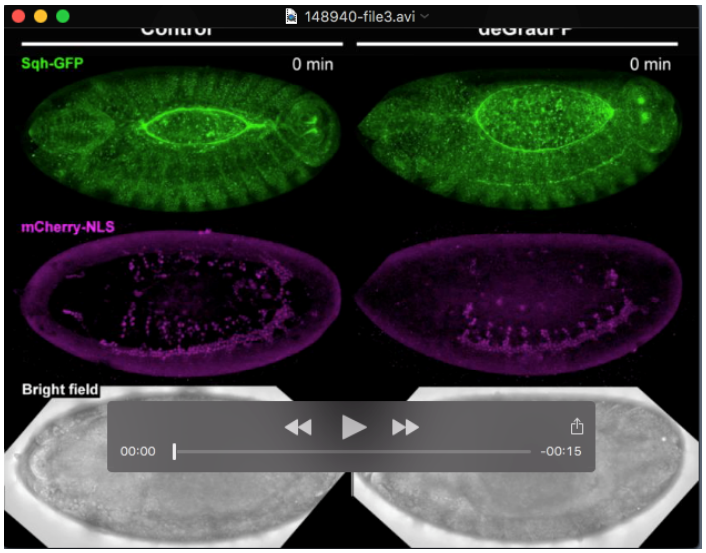

Movie 2 - Gas filling of the tracheal tubes proceeded normally in Sqh-GFP knock-down embryos

Time lapse imaging of *sqhAx3*/Y; *sqh-Sqh-GFP, btl-Gal4, UAS-mCherry*$_{NLS}$/+ control (left) and *sqhAx3*/Y; *sqh-Sqh-GFP, btl-Gal4, UAS-mCherry*$_{NLS}$*/UAS-deGradFP* Sqh-GFP knock-down (right) embryos (10min intervals, 20x objective). Gas filling of the tracheal tubes (bright field channel, bottom panels) is not impaired by knock-down of Sqh-GFP and occurs similar to control embryos approximately 5 hours past DC.

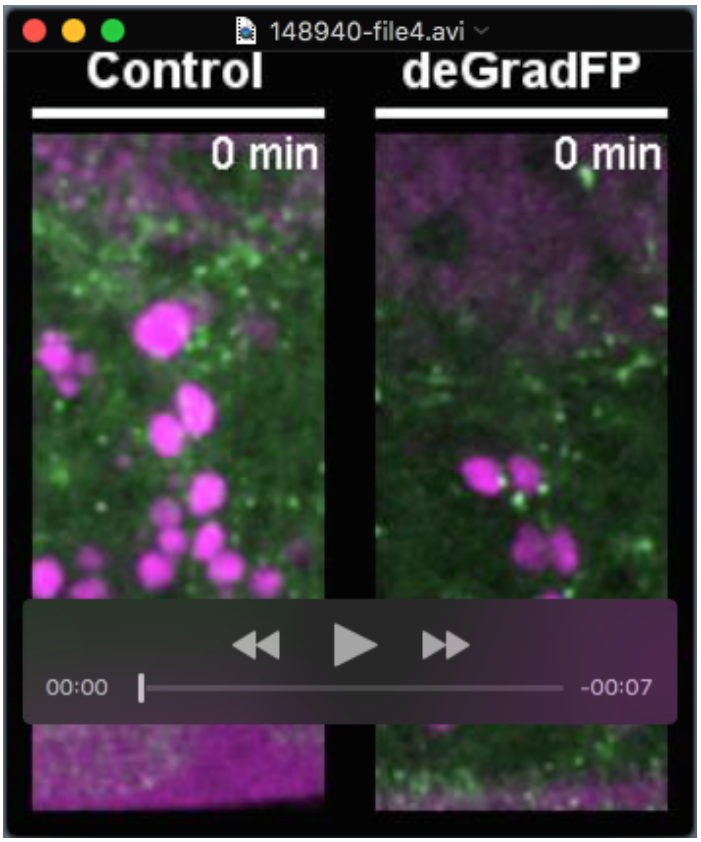

Movie 3 – DB elongation in Sqh-GFP knock-down embryos

Time lapse imaging of Tr3 DB elongation in *sqhAx3*/Y; *sqh-Sqh-GFP, btl-Gal4, UAS-mCherry*$_{NLS}$/+ control (left) and *sqhAx3*/Y; *sqh-Sqh-GFP, btl-Gal4, UAS-mCherry*$_{NLS}$/*UAS-deGradFP* Sqh-GFP knock-down (right) embryos (5min intervals, 63x objective). Tip cell migration and subsequent DB elongation is indistinguishable between Sqh-GFP knock down and control embryos.

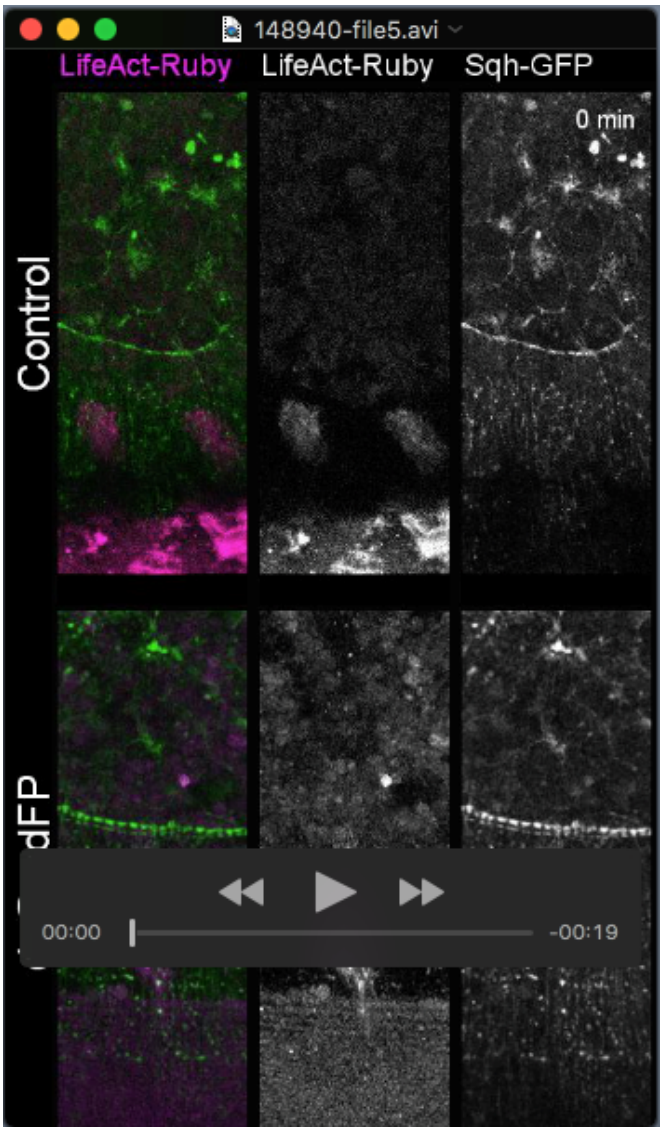

Movie 4 – Actin dynamics during DB elongation

Time lapse imaging of actin dynamics visualized by tracheal expression of Lifeact-Ruby (mangenta) during elongation of the Tr3 DB. Tip cells in both, control and deGradFP conditions, show filopodial activity, migrate dorsally and connect to the contralateral DB. Control (top): *sqhAx3*/Y; *sqh-Sqh-GFP, btl-Gal4, UAS-LifeAct-Ruby/* + and Sqh-GFP knock-down (bottom): *sqhAx3*/Y; *sqh-Sqh-GFP, btl-Gal4, UAS-LifeAct-Ruby*/*UAS-deGradFP* (2min intervals, 63x objective).